



Simulation of shear banding and crack propagation in bulk metallic glass matrix composites

G.P. Zheng*, Y. Shen

Department of Mechanical Engineering, The Hong Kong Polytechnic University, Hung Hom, Kowloon, Hong Kong

ARTICLE INFO

Article history:

Received 30 June 2010

Received in revised form 25 August 2010

Accepted 25 August 2010

Available online 3 September 2010

Keywords:

Metallic glasses

Composite

Shear band

Computer simulations

ABSTRACT

Different modes of shear banding in bulk metallic glass (BMG) matrix composites are identified from the systematic simulation studies based on a mesoscopic phase-field model for deformation in glassy alloys. We characterize the interaction between shear band and crystalline reinforcements by considering the residual stress and atomic bonding condition at the interface between BMG-matrix and the reinforcement. The simulation demonstrates that compressive residual stress assists to impede the shear bands propagating toward the reinforcements, while tensile residual stress accelerates such process. In addition, the effect of atomic bonding at the interface on shear banding is investigated by the simulation. The relations between the fracture toughness and the residual stress and atomic bonding condition at the interface are quantitatively determined.

© 2010 Elsevier B.V. All rights reserved.

1. Introduction

Bulk metallic glasses (BMGs) are promising for structural applications because of their exceptional mechanical properties such as high strength and large elastic strain, and excellent corrosion resistance [1]. But the lack of plasticity of this new class of metallic materials actually limits their applications into a few areas of functional use only. For the purpose of improving their ductility crystalline reinforcements or *in situ* formed second-phase structures can be introduced into the BMGs to form the BMG-matrix composite [2–4]. The fracture toughness and ductility of such BMG-matrix composites could be improved due to the effect of the reinforcing structures on the formation and the spreading of shear bands. Instead of catastrophic failure caused by very limited numbers of shear bands, BMG-matrix composites could show global ductility with large plastic strain because multiple shear bands are generated due to the mismatches of elasticity and thermal expansion coefficient between the reinforcement and the matrix [5]. For example, titanium–zirconium-based BMG consisting of *in situ* formed β -phase precipitates exhibits room-temperature ductility (elongation to failure) well exceeding 10 percents and large fracture toughness up to $\sim 170 \text{ MPa m}^{1/2}$ [5], which are much better than those of its monolithic counterparts. It has been shown [5] that multiple shear bands generated from and arrested by the

crystalline inclusions result in such improved tensile ductility and fracture toughness.

There are several types of BMG-matrix composites [5–7], namely, with the reinforcing structures being the *ex situ* reinforcements, *in situ* formed crystallites or second-phase amorphous alloys. In order to design these BMG-matrix composites with larger plastic strain, it is necessary to deeply understand the influence of matrix/reinforcement interfaces on shear band propagation and multiplication, especially those interfaces with sophisticated stresses states or atomic bonding conditions. However, due to the very short time scale of shear band initiation and propagation as well as the nanometer scale thickness of the interfaces, real-time observation and analysis on the effects of interfaces on shear banding seem impossible for experiment. Computer simulation can be a useful and convenient tool to study these issues, but up to date the computational modeling on these issues is still lacking.

Using Zr-based BMG with tungsten reinforcing fibers as a model system, in this work we employ phase-field modeling method [8] to analyze the effect of interface between the reinforcement and the BMG-matrix on the shear banding and crack propagation in the composite. We firstly demonstrate that such phase-field modeling approach could successfully capture all the features of shear banding and crack propagation well observed in experiments. Then the mechanical properties of the BMG-matrix composites will be quantitatively related with the stresses states and atomic bonding conditions at the matrix/reinforcement interface. The simulation could provide us with an in-depth understanding on the shear banding and cracking in BMG-matrix composite, and are extremely useful in the development and design of BMG-matrix composites for structural applications.

* Corresponding author.

E-mail address: mmzheng@polyu.edu.hk (G.P. Zheng).

2. Simulation method

As shown in Fig. 1(a), the simulation model of BMG composite consists of cylindrical reinforcing tungsten fibers with a diameter of $d=0.2\ \mu\text{m}$, which are embedded in a Zr-based BMG ($\text{Zr}_{41}\text{Ti}_{14}\text{Ni}_{10}\text{Cu}_{12.5}\text{Be}_{22.5}$) plate with edged notches. Tensile stresses perpendicular to the fibers are applied at the upper and lower edges of the plate with dimensions of $20\ \mu\text{m} \times 20\ \mu\text{m} \times 2\ \mu\text{m}$. Thus the model can be considered as a plane stress system. The physical properties of the Zr-based BMG are listed as follows [9]: glass transition temperature $T_g=625\ \text{K}$; the shear modulus $\mu=35\ \text{GPa}$; Poisson's ratio $\nu=0.35$; density $\rho_0=6050\ \text{kg/m}^3$. The elastic strain limit under uniaxial tension is $\epsilon_0=2\%$. The shear banding of BMG can be simulated by a phase-field modeling approach described in details in Refs. [8,10]. The modeling method is based on a phenomenological model for deformation of metallic glass consisting of flow defects which simply treats the formation of shear band as a consequence of the collective behavior of the structural transformation of these defects. The variable of the phase-field is the normalized free-volume density, which is defined as $\rho(\bar{\mathbf{r}}) = (v_i - v_0)/(v_m - v_0)$, where v_m is the maximum dilated volume when complete decohesion occurs at position \mathbf{r} , v_i is the atomic volume defined as the volume of the so-called Voronoi polyhedron of the i th atom, v_0 is the atomic volume in the undeformed ideal random close packing state. The governing equations for deformation defect field ρ in the BMG-matrix and displacement field \mathbf{u} can be respectively described as

$$\tau_\rho \frac{\partial \rho}{\partial t} = -\frac{\delta F}{\delta \rho} = \kappa \nabla^2 \rho - (a_0 \rho + b_0 \rho^2 + c_0 \rho^3) - \rho(a_1 + b_1 \rho)(e[\epsilon_{ij}] - e_0), \quad (1)$$

$$\rho_0 \frac{\partial^2 \bar{\mathbf{u}}}{\partial t^2} = -\nabla \left[\frac{\delta F}{\delta \epsilon_{ij}} \right] = \mu \nabla \left\{ \left[1 + \rho^2 \left(\frac{a_1}{2} + \frac{b_1}{3} \rho \right) \right] \nabla \bar{\mathbf{u}} \right\}, \quad (2)$$

where τ_ρ is the characteristic time for defect activation. κ is the surface energy of the interface between the deformation defect and defect-free region. a_0 , b_0 and c_0 , a_1 , b_1 setting in these equations are constants. $a_0=4(2-T/T_g)\Delta G$, $b_0=-32\Delta G$, $c_0=16\Delta G$; ΔG is the activation energy of flow defect in Zr-based BMG. a_1 and b_1 are set in a way to reflect the fact that the shear modulus of BMG decreases with increasing flow defect density. We define that a shear band forms in a region where $\rho > \rho_c=0.8$. For the cracking in the reinforcing crystalline fiber, as developed by Karma and Kessler [11],

the governing equation of crack field $\phi(\mathbf{r})$ describing the fracture process in the tungsten fiber can be described as

$$\tau \frac{\partial \phi}{\partial t} = D_\phi \nabla^2 \phi - V'(\phi) - \frac{\mu_0}{2} g'(\phi)(|\epsilon_{ij}|^2 - \epsilon_c^2), \quad (3)$$

where the variable ϕ would represent the crack if $\phi=1$; ϵ_{ij} is the strain tensor and μ_0 is the shear modulus of tungsten; $V(\phi)=\phi^2(1-\phi^2)/4$ and $g(\phi)=4\phi^3-3\phi^4$. $\tau=0.02\ \mu\text{s}$, $\epsilon_c=354\ \text{J/m}^2$, $D_\phi=1.02 \times 10^{-5}\ \text{J/m}$. Details of the simulation of cracking in the crystalline reinforcing fiber can be found in Ref. [12].

When the reinforcing material is introduced into BMG-matrix, due to the difference between the coefficients of thermal expansion of matrix and the reinforcing material, residual stress is inevitably introduced at the matrix/reinforcement interface, and usually can be estimated [13]. For example, in tungsten fiber-reinforced Zr-based BMG, tungsten and BMG-matrix have different thermal coefficients 4.5×10^{-6} and $8.5 \times 10^{-6}\ \text{K}^{-1}$, respectively, therefore tensile residual stress (with respect to the BMG-matrix) is likely to be introduced at the interface. However, if the reinforcement is 1080 steel fiber, compressive residual stress would be generated at the interface due to its relatively large thermal expansion coefficient $13 \times 10^{-6}\ \text{K}^{-1}$. In *in situ* formed Zr-based BMG, the lattice constant of β -phase crystallites embedded in the BMG-matrix is $0.3496\ \text{nm}$ [5], which would misfit the amorphous matrix's atomic structures, resulting in the residual stress and free-volume defect ($\rho \neq 0$) at the interface as well.

The residual stresses at the interface are quantitatively considered in Eq. (2) based on the boundary conditions (BCs) for the displacement field \mathbf{u} at the interface:

$$\mathbf{n} \cdot [(c\nabla \mathbf{u} + \mathbf{a}\mathbf{u} - \gamma)_1 - (c\nabla \mathbf{u} + \mathbf{a}\mathbf{u} - \gamma)_2] = \mathbf{g} \quad (4)$$

where c is the module matrix, \mathbf{n} is the direction vector and \mathbf{g} is the residual stress at the matrix/reinforcement interface; parameters in bracket 1 are for the BMG-matrix, and 2 for the reinforcing material. In our simulation we set parameters a and γ as zero. Fig. 2(a) and (d) shows the displacement field \mathbf{u} around the matrix/reinforcement interface when there are compressive and tensile residual stresses at the interface, respectively. Dirichlet boundary condition for Eq. (1) is imposed for ρ at the interface, i.e., ρ is a constant w at the interface. Because the deformation defect field ρ describes atomic volume dilatation in the BMG-matrix, hence w measures the atomic bonding condition between the amorphous matrix and the crystalline reinforcing materials, e.g., for perfect atomic bonding $w=0$, and $w=1$ for the decohesion between the BMG-matrix and the reinforcement.

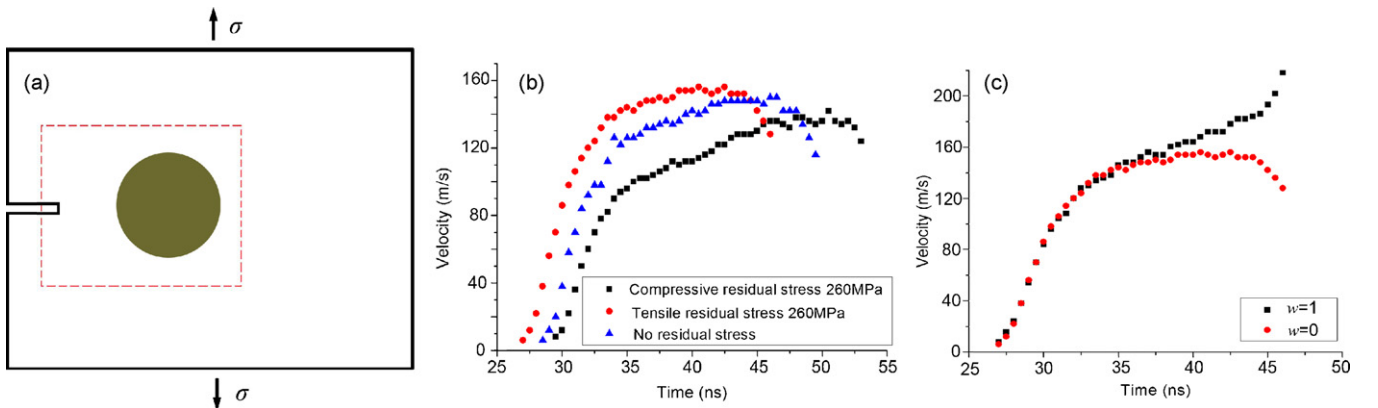


Fig. 1. (a) A system for the simulation of shear banding in BMG, the shadow area represents reinforcing fiber; (b) effect of residual stress at the interface on the velocity of shear band propagating toward the fiber; (c) effect of atomic bonding condition at the interface on the velocity of shear band propagating toward the fiber. The stress intensity factor is $K_I=27.5\ \text{MPa m}^{1/2}$ for each case. The distance between the notch and the interface is $0.28\ \mu\text{m}$.

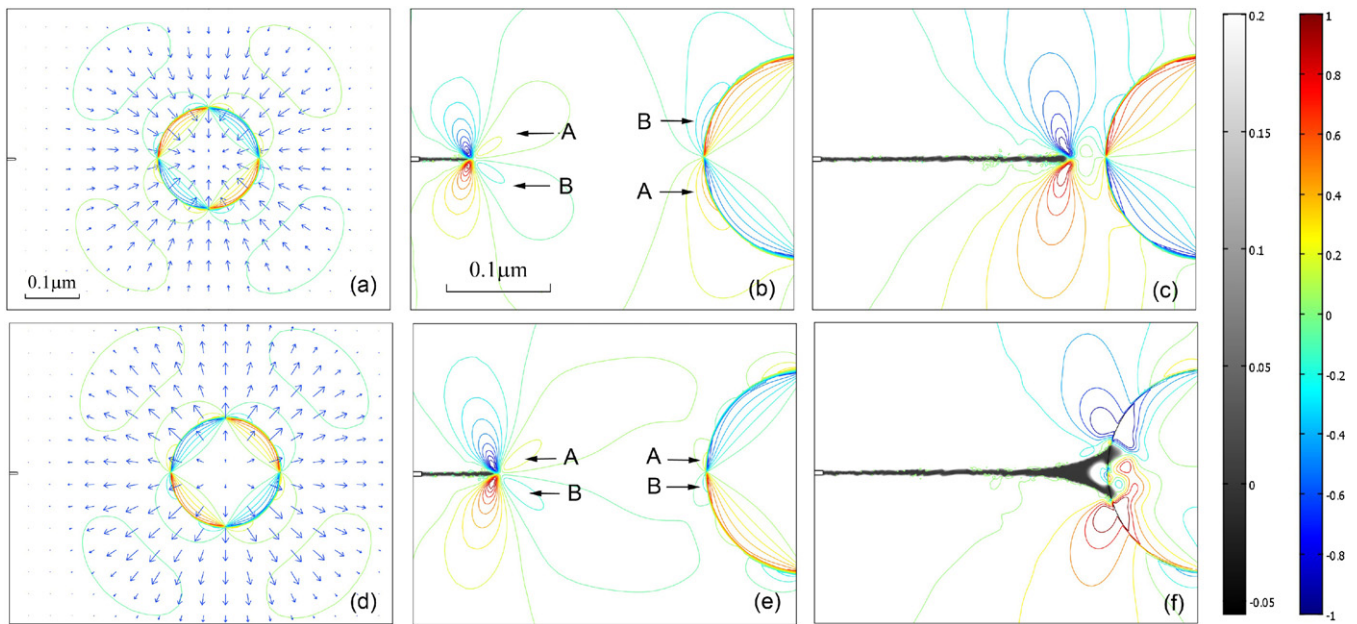


Fig. 2. (a)–(c) Shear band propagates toward the reinforcing fiber with a compressive residual stress -260 MPa at its interface at 5, 35 and 50 ns, respectively; (d)–(f) shear band propagates toward the reinforcing fiber with a tensile residual stress 260 MPa at its interface at 5, 35 and 50 ns, respectively. The arrows in (a) and (d) represent the displacement fields. The gray scales correspond to the values of $1 - \rho$ in the matrix; or to the value of $1 - \phi$ in the tungsten fiber; the contour plots with the color bars ($\times 870$ MPa) are for shear stresses τ in the composite. The arrows A and B in (b) and (e) indicate the negative and positive shear stresses, respectively.

3. Result and discussion

As shown in Fig. 1(b), tensile residual stress at the interface would accelerate the propagation of shear band in the BMG-matrix, while the compressive residual stress would slow it down. These results are quite consistent with the previous experimental study conducted by Conner et al. [6], who predicted that tensile hoop stress around the interface would encourage the cracks to propagate toward the reinforcing fibers, while compressive hoop stress should deflect cracks away from the fibers. Our phase-field simulation results provide further insight views on how these two opposite residual stresses at the matrix/reinforcement interface affect the shear band propagation. If there is compression residual stress at the interface, the shear stress around the shear band approaching the reinforcement has the opposite sign as that around the reinforcement, as shown in Fig. 2(b) and (c). Hence shear band propagation will be decelerated (Fig. 2(c)) and even forced to detour around the reinforcement. If there is tensile residual stress at the interface, the shear stress around the shear band approaching the reinforcement has the same sign as that around the reinforcement, as shown in Fig. 2(e) and (f). As a consequence the shear band will be accelerated to propagate toward the interface (Fig. 2(e)) and eventually triggers cracks in the crystalline reinforcement, as shown in Fig. 2(f).

Compressive residual stress not only hinders shear band propagation, but also affects the initiation of shear band from the initial single-edge notch. Fig. 3 shows the relation between the fracture toughness and the compressive residual stress g at the interface, when the minimum distance between the notch and the reinforcement is fixed as $0.28 \mu\text{m}$. For the compressive residual stress g smaller than $g_0 = 195$ MPa, its influence on the shear band initiation is negligible. If g is larger than 195 MPa, the fracture toughness of the composite K_{IC} can be described as

$$K_{IC} = K_{IC0} + 0.017|g - g_0|, \quad (5)$$

where $K_{IC0} = 22 \text{ MPa m}^{1/2}$ is the fracture toughness for shear band initiation from the notch in BMG without the reinforcement.

Based on these simulation results we can conclude that the tensile residual stress at the matrix/reinforcement interface is preferable for enhancing the plasticity of the BMG composite [14,15], since the reinforcement in this case may accommodate local plastic strain triggering by the shear band, as shown in Fig. 2(f). Compressive residual stress would improve the fracture toughness of BMG-matrix, but it is no helpful for enhancing the plasticity of BMG. This is because shear band impeded by the reinforcement tends to detour around the reinforcement as shown in Fig. 4(c), resulting in the delamination and pullout of the reinforcements during the fracture process in the BMG-matrix composite.

Fig. 1(c) shows the effect of atomic bonding condition at the matrix/reinforcement interface on shear banding in the BMG-matrix without considering the residual stress at the interface ($g=0$). When the shear band approaches the interface with the

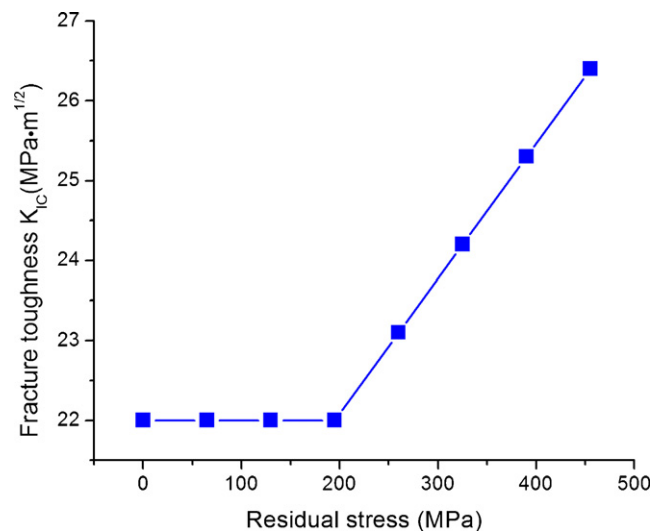


Fig. 3. The relation between the fracture toughness of BMG composite and the compressive residual stress at the interface.

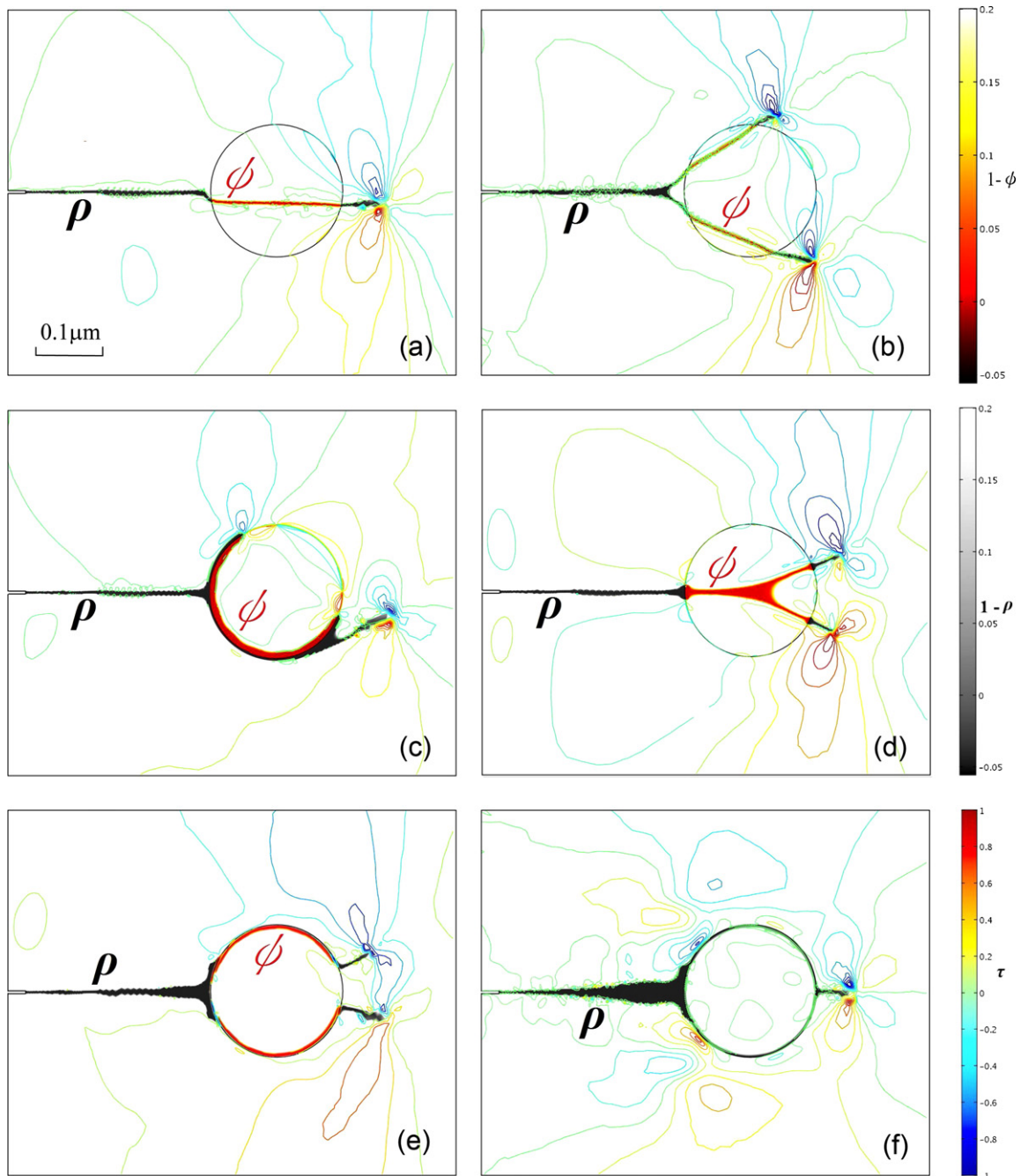


Fig. 4. Different deformation modes for shear banding and crack propagation in the BMG composite: (a) and (b) Shear banding induced cracking inside the reinforcement after the shear band interacts with reinforcement. $g=0$, $w=0$; $K_I=24.2 \text{ MPa m}^{1/2}$ (a), and $27.5 \text{ MPa m}^{1/2}$ (b); (c) propagation of shear band along the reinforcement surface with compressive residual stress $g=-435 \text{ MPa}$; $w=0$; (d) shear banding induced cracking inside the reinforcement with tensile residual stress $g=175 \text{ MPa}$ at its surface; $w=0$; (e) Branching of shear band along the reinforcement surface; $w=0.8$; $g=0$. (f) Shear banding at opposite sides of the reinforcement surface; $w=1$; $g=0$. $K_I=27.5 \text{ MPa m}^{1/2}$ in (c)–(f). The defect field ρ in BMG and crack field ϕ in tungsten is identified and their values are indicated by grey scales and color scales, respectively.

worse bonding condition ($w=1$), its propagation will be speeded up. If the interface has the perfect bonding condition ($w=0$), shear band propagation will slow down. On the other hand shear bands can be initiated from the interface if the bonding condition at the interface satisfies $0.6 < w < 1$ [10]. In this case the fracture toughness of the BMG composite is quantitatively related with the atomic bonding condition at the interface as

$$K_{IC} - K_{IC0} \propto (1-w)^b \quad (6)$$

where $b=1.6$.

The effects of residual stress and atomic bonding condition at the matrix/reinforcement interface on shear banding and crack

propagation can be summarized into several deformation modes as shown in Fig. 4. If the interface between the BMG-matrix and the reinforcement has perfect adhesion ($w=0$), without residual stress ($g=0$) shear band touching the interface would cause cracking inside the crystalline reinforcement, shown as color plots for ϕ in Fig. 4(a) and (b). Larger applied load would trigger shear band to split in front of the reinforcement to suspend more plastic strains as shown in Fig. 4(b). With compressive residual stress ($g=-435 \text{ MPa}$) at the interface, shear banding tends to occur along the surface of the reinforcement as shown in Fig. 4(c). With tensile residual stress ($g=175 \text{ MPa}$) at the interface, there is a straight propagation of the shear band before it touches the interface,

resulting in the cracking inside the reinforcement as shown in Fig. 4(d).

For the interface with defective atomic bonding condition ($0 < w < 1$), the shear band would split into two branches and detour around the reinforcing fiber as shown in Fig. 4(e). Furthermore, in the worse atomic bonding condition at the interface ($w = 1$), shear band propagation immediately transfers from one side of the reinforcement to the other side without any branching as shown in Fig. 4(f).

The above-mentioned deformation modes have been experimentally discovered in BMG composites [2–7,13–15]. Our simulations can quantitatively describe the occurrences of these deformation modes by characterizing the residual stresses and atomic bonding condition at the matrix/reinforcement interface, e.g., through Eqs. (4)–(6). Therefore the simulation approach developed in this study is extremely useful in the development and design of BMG-matrix composites with improved fracture toughness and ductility.

4. Conclusions

Phase-field modeling was employed to study shear banding and crack propagation in the Zr-based BMG composites. It is found the tensile residual stress at the interface between BMG-matrix and the reinforcement is preferred for the purpose of enhancing the plasticity of the BMG composite, while the compressive residual stress would improve its fracture toughness. Furthermore, the residual stress and atomic bonding condition at the interface can be used to determine the deformation modes in the BMG-matrix composite. The simulation results are all consistent with those from the experimental investigations, suggesting that the modeling could provide guidance for materials selection and preparation for high-performance BMG composites. Based on the simulation it is feasible

to design and prepare either fiber-reinforced or *in situ* formed BMG-matrix composites where major shear band propagating in the BMG-matrix interacts with the reinforcement, resulting in multiple shear bands or secondary shear bands or plastic deformation of the crystalline reinforcement which accommodate more plastic strains in the composites.

Acknowledgements

The work described in this paper was supported by a grant from the Research Grants Council of the Hong Kong Special Administrative Region, China (Project No. PolyU 7196/06E). The authors are grateful for the supports provided by the Research Funds of Hong Kong Polytechnic University (Project No. A-SA29).

References

- [1] C.J. Byrne, M. Eldrup, *Science* 321 (2008) 502–503.
- [2] C. Fan, C.F. Li, A. Inoue, V. Haas, *Phys. Rev. B* 61 (2000) R3761–R3763.
- [3] M.H. Lee, D.J. Sordelet, *Appl. Phys. Lett.* 88 (2006) 261902.
- [4] J.G. Lee, D.-G. Lee, S. Lee, N.J. Kim, *Metall. Mater. Trans.* 35A (2004) 3753–3761.
- [5] D.C. Hofmann, J.-Y. Suh, A. Wiest, M.-L. Lind, M.D. Demetriou, W.L. Johnson, *PNAS* 105 (2008) 20136–20140.
- [6] R.D. Conner, R.B. Dandliker, W.L. Johnson, *Acta Mater.* 46 (1998) 6089–6102.
- [7] A. Concustell, N. Mattern, H. Wendrock, U. Kuehn, A. Gebert, J. Eckert, A.L. Greer, J. Sort, M.D. Baró, *Scripta Mater.* 56 (2007) 85–88.
- [8] G.P. Zheng, M. Li, *Phys. Rev. B* 80 (2009) 104201.
- [9] H.A. Bruck, T. Christman, A.J. Rosakis, W.L. Johnson, *Scripta Metall. Mater.* 30 (1994) 429.
- [10] Y. Shen, G.P. Zheng, *Scripta Mater.* 63 (2010) 181–184.
- [11] A. Karma, D.A. Kessler, *Phys. Rev. Lett.* 87 (2001) 045501.
- [12] G.P. Zheng, Y. Shen, *Int. J. Solids Struct.* 47 (2010) 320.
- [13] U. Kühn, J. Eckert, N. Mattern, L. Schultz, *Appl. Phys. Lett.* 80 (2002) 2478–2480.
- [14] Y.C. Kim, E. Fleury, J.-C. Lee, D.H. Kim, *J. Mater. Res.* 20 (2005) 2474–2479.
- [15] D.C. Hofmann, J.-Y. Suh, A. Wiest, G. Fuan, M.-L. Lind, M.D. Demetriou, W.L. Johnson, *Nature* 451 (2008) 1085–1089.